# Chapter 3

# A General Approach to Detect Protein Expression *In Vivo* Using Fluorescent Puromycin Conjugates

This chapter has previously appeared as: S.R. Starck, H.M. Green, J. Alberola-Ila, R.W. Roberts. A General Approach to Detect Protein Expression *In Vivo* using fluorescent puromycin conjugates. *Chem. Biol.* In press.

## Abstract

Understanding the expression of known and unknown gene products represents one of the key challenges in the post-genomic world. Here, we have developed a new class of reagents to examine protein expression *in vivo* that does not require transfection, radiolabeling, or the prior choice of a candidate gene. To do this, we constructed a series of puromycin conjugates bearing various fluorescent and biotin moieties. These compounds are readily incorporated into expressed protein products in cell lysates *in vitro* and efficiently cross cell membranes to function in protein synthesis *in vivo* as indicated by flow cytometry, selective enrichment studies, and western analysis. Overall, this work demonstrates that fluorescent-puromycin conjugates offer a general

means to examine protein expression *in vivo*.

## 3.1 Introduction

Complete sequencing of the human genome (1, 2) shows that less than 50% of the putative gene transcripts correspond to known proteins. A complete understanding of the proteome awaits the identification of thousands of unassigned gene products and assignment of their role in signaling cascades (3), membrane trafficking (4), apoptosis (5), and other cellular processes. Currently, there are large-scale techniques to study cellular protein levels indirectly using DNA and mRNA arrays (6). However, these techniques do not directly monitor the level of protein synthesis. Methods to directly monitor protein expression *in vivo* are extremely useful, particularly in the study of higher organisms with many different cell and tissue types.

Currently, protein expression is studied using pulse-labeling with a radioactive tracer or by transformation with fluorescent reporters based on the green fluorescent protein (GFP) and mutants (BFP, CFP, and YFP) (7). Pulse-labeling experiments typically require the cell(s) to be destroyed and are not amenable to microscopy experiments with simultaneous protein synthesis detection. Genetically encoded GFP mutants and fusion proteins have seen broad biological applications including study of $Ca^{2+}$ localization (8) protein tyrosine kinase activity (9), and mRNA trafficking and protein synthesis localization in cultured neurons (10, 11). However, the use of GFP-based constructs is limited to cells that can be efficiently transfected. Additionally, DNA transfection protocols often require several days to produce cells yielding robust GFP-based fluorescent signals and also inundate the protein synthesis machinery with a non-native transcript due to the use of strong upstream promoters. Finally, transfection-based strategies generally require choice of a particular candidate gene product.

We reasoned that puromycin-based reagents might provide a general means to ex-

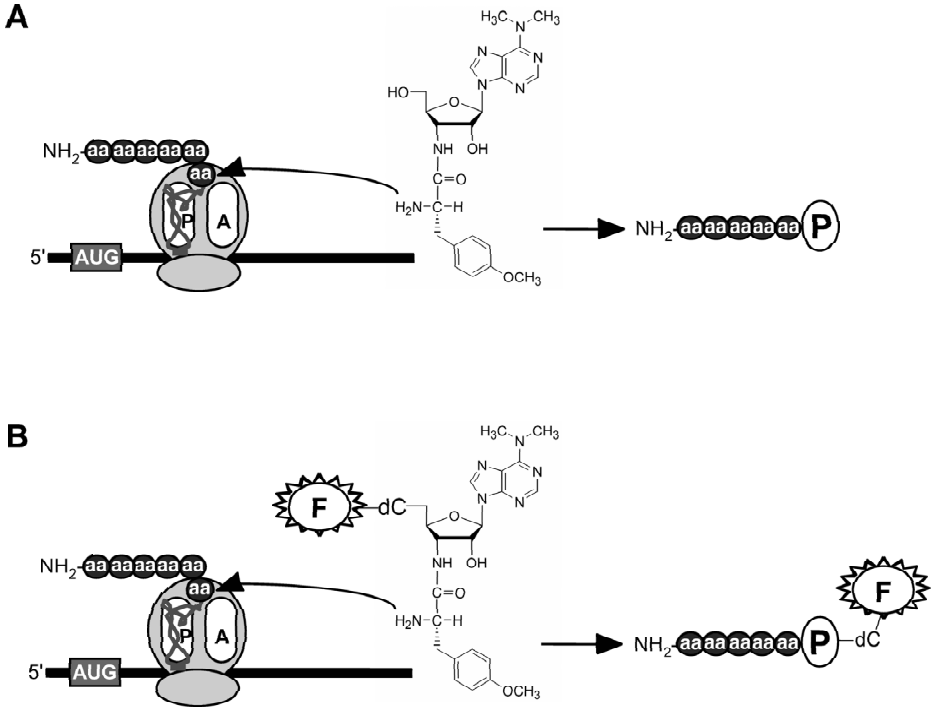


Figure 3.1: (A) Puromycin (**P**) participates in peptide bond formation with the nascent polypeptide chain. (B) Puromycin-dye conjugates, of the form X-dC-puromycin where X = fluorescein (**F**), are also active in translation and become covalently linked to protein.

amine protein expression. Puromycin is a structural analogue of aminoacylated-tRNA (aa-tRNA) and participates in peptide-bond formation with the nascent polypeptide chain (Figure 3.1A) (12, 13). Previously, various puromycin derivatives of the form X-dC-puromycin have been examined and shown to be functional during *in vitro* translation experiments (14, 15, 16, 17). In principle, a fluorescent or biotinylated variant of puromycin should be functional in protein synthesis *in vivo* if it is able to enter cells in a non-destructive fashion (Figure 3.1B). In this way, selective labeling of newly synthesized proteins would enable direct monitoring of protein expression

and provide the potential for both spatial and temporal resolution.

Here, we demonstrate that a variety of puromycin conjugates can be used as detectors of protein synthesis in live cells. This work shows that puromycin conjugates can easily enter cells and covalently label newly synthesized proteins, enabling direct detection of protein expression *in vivo*.

## 3.2 Results

### 3.2.1 Design of Puromycin Conjugates

To label newly synthesized proteins, our puromycin conjugates would have to satisfy three general criteria: 1) functionality in peptide bond formation, 2) cell permeability, and 3) ready detection in a cellular or biochemical context. In addressing the first issue, it had been previously shown that puromycin derivatives bearing substitutions directly off the 5'-OH functioned poorly *in vitro* (e.g., biotin-puromycin $IC_{50} = 54\,\mu M$) (17), whereas conjugates with the general form X-dC-puromycin (e.g., biotin-dC-puromycin) were substantially more effective ($IC_{50} = 11\,\mu M$) (17). We therefore chose to design molecules by varying the substituents appended to dC-puromycin (Figure 3.2A).

In order to facilitate cellular entry and detection, we considered a number of factors including 1) type and position of the label, 2) the linker between the label and dC-puromycin, 3) background fluorescence properties, and 4) membrane permeability including net charge and hydrophobicity. We then designed and synthesized various dC-puromycin conjugates to address these issues systematically. The first series of puromycin conjugates (**1**, **3**, **4**, **6**, **8**; Figure 3.2A) either contain fluorescent dyes (compounds **1** and **4**), biotin (compound **6**), or both (compounds **3** and **8**). Two different fluorescent dyes were utilized ($Cy_5$ and fluorescein) to provide detection at a range of emissions. Biotin labels were introduced to enable detection via western blot analysis or affinity purification. We also prepared a series of compounds ( **2**, **5**,

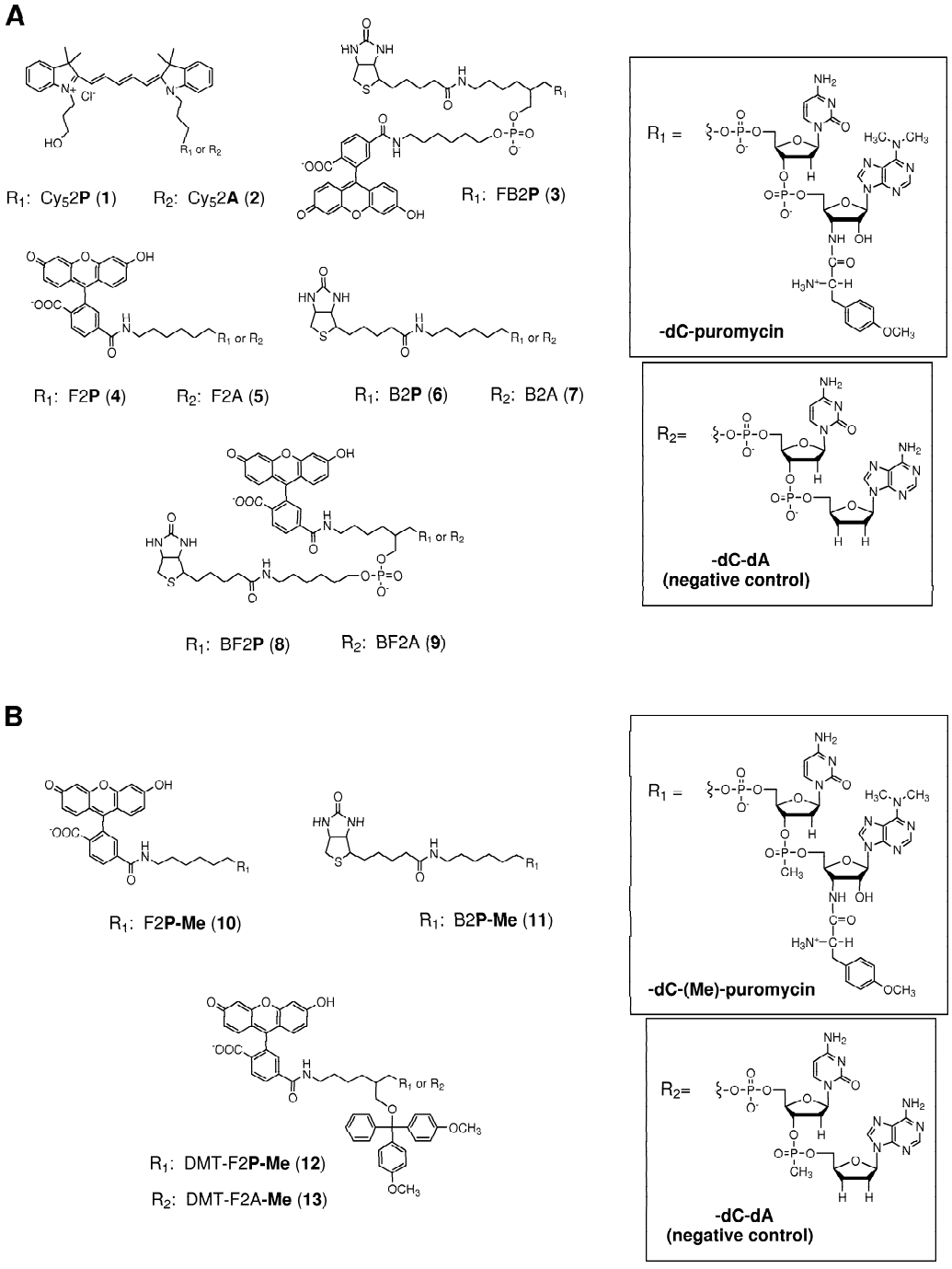


Figure 3.2: (A) Structure of puromycin conjugates and negative control conjugates. (B) Structure of phosphonate-based conjugates.

**7**, **9**; Figure 3.2A), which lack the 3'-amino acid moiety to serve as negative controls.

A second series of conjugates with a phosphonate linkage between dC and puromycin were prepared to examine whether reduction of charge would enhance cell membrane solubility and facilitate cellular entry (Figure 3.2B). Three compounds (**10**, **11**, **12**; Figure 3.2B) were constructed bearing fluorescein (**10**, F2**P**-Me), biotin (**11**, B2**P**-Me), or the hydrophobic dimethoxytrityl group (DMT) and fluorescein (**12**, DMT-F2**P**-Me). A DMT bearing fluorescein-dC-dA conjugate (DMT-F2A-Me) served as a negative control (**13**; Figure 3.2B). The DMT group was added to gauge whether the addition of a hydrophobic group would further enhance entry into cells.

### 3.2.2 Analysis of Puromycin-conjugate Activity *In Vitro*

We began our analysis by examining the activity of each of our conjugates *in vitro* for their ability to inhibit protein translation. Previously, we had used this activity assay to measure the $IC_{50}$ for various puromycin conjugates (17) and analogs (18), as well as demonstrate a direct relationship between the $IC_{50}$ and the efficiency of protein labeling (17). Using this approach, we measured $IC_{50}$ values for the compounds in Figure 3.2A and 3.2B (Figure 3.3A). High resolution SDS-tricine gel data corresponding to a typical $IC_{50}$ determination is shown for $Cy_5$2**P** (**1**) and $Cy_5$2A (**2**) (Figure 3.3B). Generally, the activity of conjugates with the form X-dC-puromycin falls over a fairly narrow range *in vitro*, with $IC_{50}$ values ranging from ~4 to ~30 $\mu$M (Table 3.1). Also, control conjugates that lack the amino acid moiety, e.g., $Cy_5$2A (**2**) and BF2A (**9**), show little ability to inhibit protein synthesis even at high concentrations.

We next wished to confirm that our puromycin conjugates could become covalently attached to protein *in vitro*. To do this, we translated globin mRNA in the presence of increasing concentrations of FB2**P** (**3**), a conjugate containing fluorescein and biotin moieties (Figure 3.4A). Next, the concentration-dependent incorporation of FB2**P** was analyzed using neutravidin affinity chromatography of these same translation reactions (Figure 3.4B). These data indicate that puromycin conjugates are incorpo-

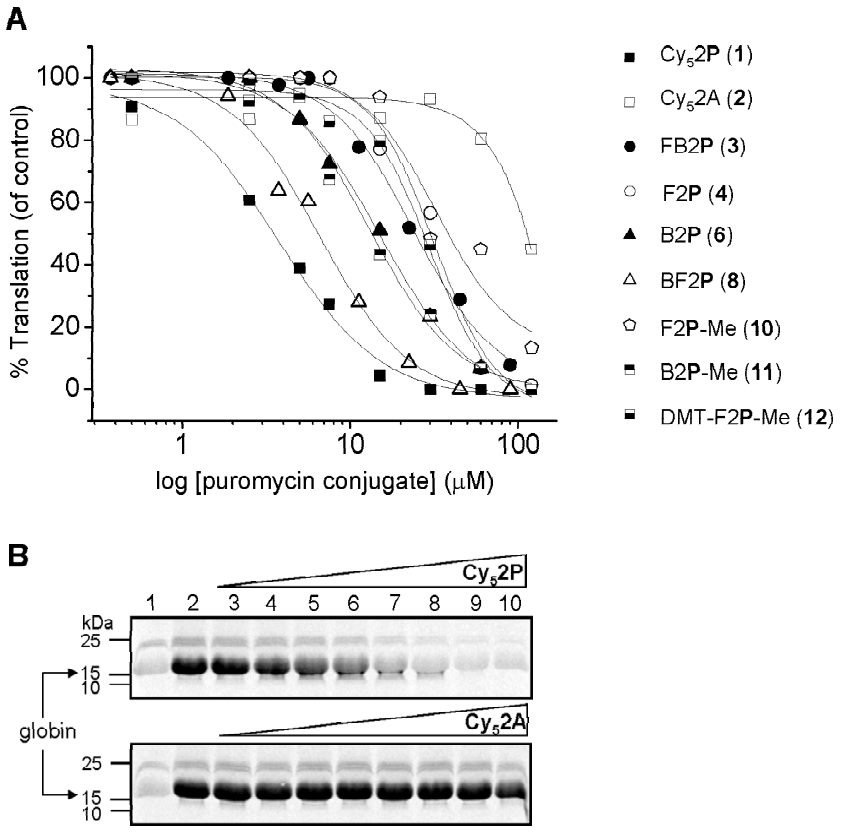


Figure 3.3: *In vitro* $IC_{50}$ determination for puromycin conjugates. (A) Percent of globin translation relative to the no conjugate control for compounds **1**, **2**, **3**, **4**, **6**, **8**, **10**, **11**, **12**. (B) Tricine-SDS-PAGE analysis of globin translation reactions in the presence of $Cy_5$2**P** (**1**) (top) and $Cy_5$2A (**2**) (bottom): Lane 1, no template and no conjugate; lane 2, globin alone; lanes $3-10$, conjugate concentrations from 0.5 to 120 $\mu$M.

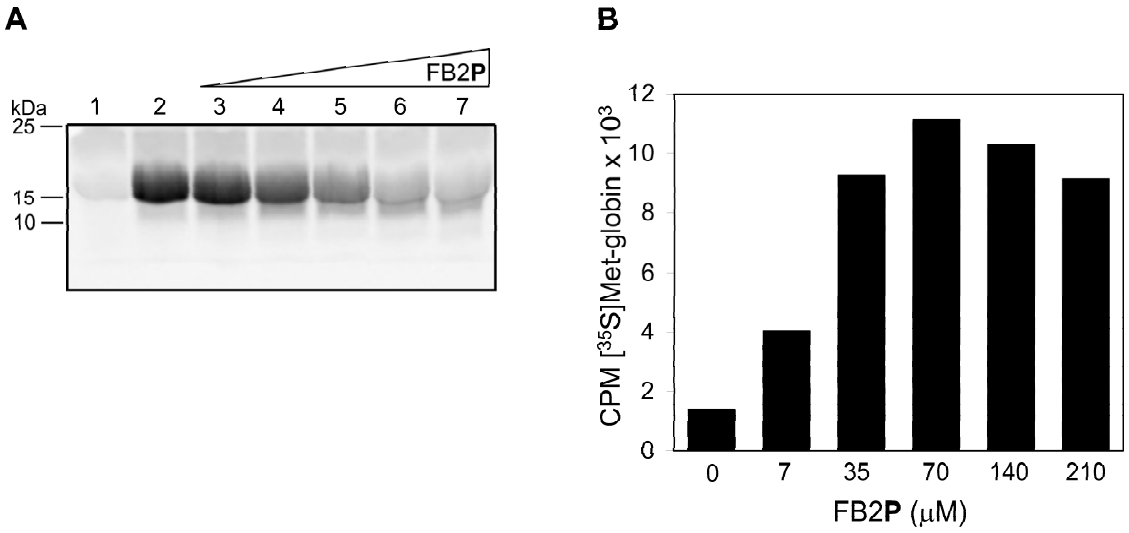


Figure 3.4: Protein labeling with the fluorescent puromycin conjugate FB2P (**3**). (A) Tricine-SDS-PAGE analysis of globin translation reactions incubated with increasing concentrations of **3**: Lane 1, no template, no conjugate; lane 2, globin alone; lane 3, 7 $\mu$M; lane 4, 35 $\mu$M; lane 5, 70 $\mu$M; lane 6, 140 $\mu$M; and lane 7, 210 $\mu$M. (B) Neutravidin-purified globin-FB2**P** complexes from translation reactions in (A).

| Conjugate | $IC_{50}$ ($\mu$M) |
|---|---|
| (**1**) $Cy_5$2**P** | 3.8 |
| (**2**) $Cy_5$2A | >100 |
| (**3**) FB2**P** | 24 |
| (**4**) F2**P** | 22 |
| (**5**) F2**P**-Me | 25 |
| (**6**) DMT-F2**P** | 29 |
| (**7**) BF2**P** | 5.8 |
| (**8**) B2**P** | 15 |
| (**9**) B2**P**-Me | 16 |

Table 3.1: The concentration of puromycin conjugate required for 50% inhibition of globin translation ($IC_{50}$). In replicate experiments, the standard error is <5%).

rated efficiently over a broad concentration range ranging from 2- to 3-fold below the $IC_{50}$ to well above it. Thus labeling is possible even at concentrations where protein synthesis is not greatly inhibited.

These observations support the development of a broad range of puromycin-based reagents for two reasons. First, compounds of the form X-dC-puromycin appear tolerant to a wide variety of substitutions, including molecules containing more than one detection handle (e.g., BF2**P** and FB2**P**). Interestingly, even the methyl phosphonate versions (F2**P**-Me, **10**; B2**P**-Me, **11**; DMT-F2**P**-Me, **12**) showed good levels of *in vitro* activity. Second, the $IC_{50}$ values indicate that even modest concentrations of each of these reagents in the low micromolar range will be sufficient to achieve good levels of protein labeling. This is because our data here (Table 3.1; Figures 3.3 and 3.4) as well as previous data (17, 18), demonstrate that protein labeling is achieved at or below the $IC_{50}$ value. Thus, these *in vitro* translation and protein labeling assays provide a starting concentration range for analysis in live cells.

### 3.2.3 Analysis of Puromycin-conjugate Activity *In Vivo*

In order to analyze the activity of puromycin conjugates *in vivo*, we needed to choose both an appropriate cell line and an appropriate quantitation and detection scheme. While microscopy is a powerful means to analyze individual cells and small sections of tissue, we wished to perform experiments where thousands to millions of cells could be examined for protein labeling. We therefore chose flow cytometry as our primary means to analyze uptake and incorporation of our conjugates. In addition to providing a quantitative measure of fluorescence and cell size, flow cytometry methods enable live cells and dead cells to be readily distinguished (19). We chose the mammalian thymocyte D9 cell line (16610D9) (20) for our experiment for four reasons: 1) they have relatively uniform size and shape, 2) they do not aggregate, making single cell detection possible, 3) they are suspension cells, which allows for ready growth in culture with subsequent acquisition of a large number of single cell readings using flow cytometry and 4) they are amenable to routine infection techniques to introduce selectable markers and GFP-based tags.

We began by comparing the concentration and time dependence of labeling with F2**P** (**4**) and the negative control conjugate F2A (**5**) (Figure 3.5A,B). For F2**P**, progressively increased fluorescence is seen with increasing time (Figure 3.5A,B) and the greatest enhancement is seen after the 24 h incubation at both 5 $\mu$M and 25 $\mu$M of the conjugate. At both concentrations, a substantial population of live cells is detected and demonstrates up to 4-fold enhanced fluorescence relative to the F2A control molecule. Longer incubation (48 hours) in the presence of F2**P** eventually kills the majority of cells at both concentrations tested. In contrast, the background fluorescence from F2A reaches a maximum of $\sim 10^1$ units after a 7 h incubation for both 5 and 25 $\mu$M incubations (Figure 3.5A,B) and F2A has no apparent effect on cell viability. The fluorescence enhancement beyond $10^1$ units for cells treated with F2**P** is consistent with C-terminal protein labeling by the fluorescein-puromycin conjugate. These experiments also suggest that there is an optimum concentration

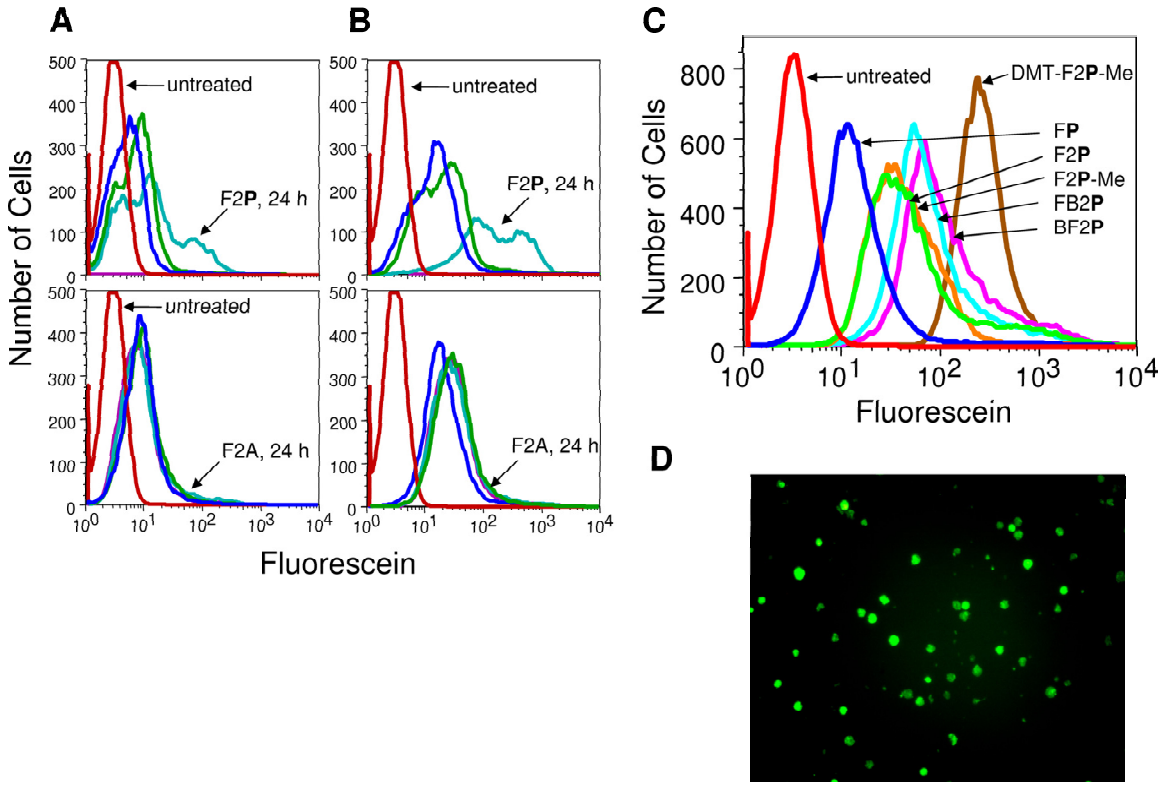


Figure 3.5: Analysis of puromycin conjugate activity in D9 thymocyte cells. Dose-response analysis of D9 thymocyte cells treated with F2**P** or F2Λ at (Λ) 5 $\mu$M and (B) 25 $\mu$M. Incubation times are 1 (■), 7 (■), 24 (■), and 48 h (■). Untreated cells incubated for 1h are indicated with (■). Cells were analyzed using a flow cytometer and gated on a live cell population according to forward and side scatter plots. (C) Flow cytometry analysis of untreated cells (■); Fluorescein-puromycin, F**P** (■); F2**P**, **4** (■); F2**P**-Me, **10** (■); FB2**P**, **3** (■); BF2**P**, **8** (■); DMT-F2**P**-Me, **12** (■). Cells were incubated for 24 h with puromycin conjugates at 50 $\mu$M. Analysis was performed using flow cytometry using a live cell gate as in Λ and B. (D) Epi-fluorescence microcopy of D9 cells treated with DMT-F2P-Me (25 $\mu$M) with 200 X magnification.

and incubation time for labeling expressed proteins without killing the cells.

We next wanted to examine the relative level of fluorescence enhancement for a series of conjugates. To do this, a uniform population of D9 cells was split into separate containers, each containing identical concentrations of a different puromycin conjugate, incubated for 24 hours, and analyzed by flow cytometry with a live-cell gate as before (Figure 3.5C). In this series, DMT-F2**P**-Me (**12**) gives the strongest enhancement and the rank order of compounds follows DMT-F2**P**-Me (**12**) > FB2**P** (**3**) ~ BF2**P** (**8**) > F2**P** (**4**) ~ F2**P**-Me (**10**) > F**P**. The $IC_{50}$ values for all the compounds with the exception of F**P** ($IC_{50}$ = 120 $\mu$M (17)) are relatively similar, while addition of the DMT group in compound (**12**) would be expected to confer increased hydrophobicity and membrane permeability. Compounds containing a phosphate (F2**P** (**4**)) or a methylphosphonate (F2**P**-Me (**10**)) bridging the puromycin and dC residue show little difference in $IC_{50}$ (Figure 3.3 and Table 3.1) and *in vivo* labeling (Figure 3.5C), arguing that charge at this position does not play a key role in either the activity as a substrate or entry into the cell. The poor $IC_{50}$ for F**P** *in vitro* (17) correlates with the small fluorescence enhancement seen for this compound *in vivo* (Figure 3.5C). Epi-fluorescence microscopy confirms that the conjugate DMT-F2**P**-Me (**12**) readily enters and labels D9 cells brightly (Figure 3.5D).

Following these experiments, we next wished to confirm that two of the best compounds, BF2**P** (**8**) and DMT-F2**P**-Me (**12**) also showed fluorescence enhancement *in vivo* relative to control molecules containing only a terminal adenosine. Indeed, comparison of cells treated with BF2**P** (**8**) versus BF2A (**9**) (Figure 3.6A) and DMT-F2**P**-Me (**12**) versus DMT-F2A-Me (**13**) (Figure 3.6B), indicates that compounds bearing the terminal puromycin moiety show a 3- to 4-fold fluorescence enhancement as compared with the control molecules.

This shift in fluorescence is consistent with labeling protein during rounds of translation. Overall, the combination of our *in vitro* and *in vivo* observations is consistent with the notion that the overall fluorescence enhancement reflects both

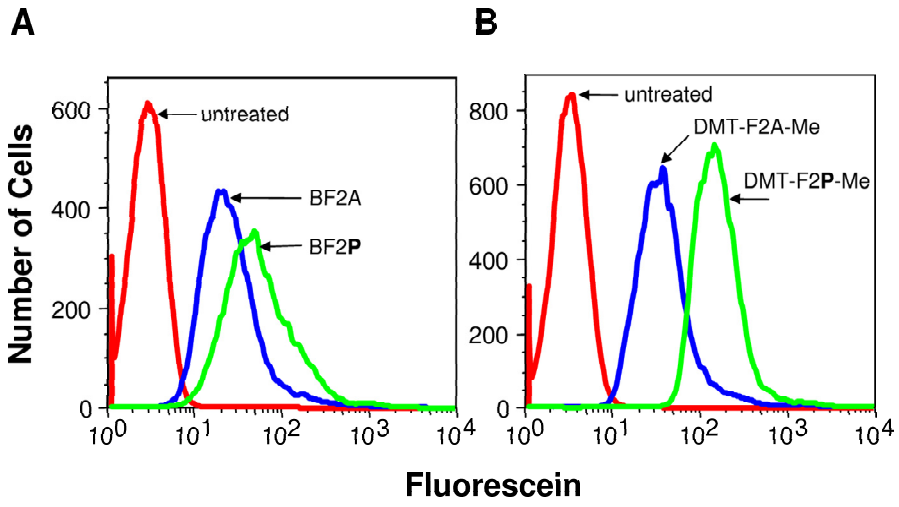


Figure 3.6: Fluorescence shift analysis for puromycin conjugates versus negative control molecules in D9 thymocyte cells. (A) Untreated cells (■); BF2A, **9** (■); BF2**P**, **8** (■). (B) Untreated cells (■); DMT-F2A-Me, **13** (■); DMT-F2**P**-Me, **12** (■). Analysis was performed using flow cytometry using a live cell gate as described for Figure 3.5.

the efficacy and the cellular permeability of the compounds.

### 3.2.4 Mechanism of Puromycin Conjugate Activity *In Vivo*

We next wished to demonstrate that the puromycin conjugates we had constructed were acting *in vivo* by the same mechanism as puromycin itself. Puromycin can be used as a selection agent in mammalian cell culture to kill cells that lack the resistance gene encoding puromycin *N*-acetyl-transferase (PAC) (21). This enzyme *N*-acetylates the reactive amine on puromycin and blocks its ability to participate in peptide bond formation (22, 23). In a mixed population of cells, those that lack a vector expressing PAC can be selectively killed by long incubations (>48 hours) with puromycin, leaving only vector-containing cells alive. Previously, we showed that chemical acylation inactivates puromycin-mediated translation inhibition *in vitro* (17). Thus, we wished to see if the D9 cells bearing PAC would be resistant to killing (and thus enriched in the mixed population) by long incubations with puromycin itself or our puromycin conjugates *in vivo*.

Foreign genes can be inserted into D9 cells by infection with a viral vector (see Experimental Procedures). Vectors that express GFP provide a straightforward means to measure the fraction of cells that become infected and a direct means to monitor any vector-mediated enrichment. We infected D9 cells with a viral vector driven by a mouse stem cell virus promoter (MSCV) containing an internal ribosome entry site (IRES) upstream from enhanced green fluorescent protein (EGFP) referred to as MIG (MIG = MSCV-IRES-GFP; Figure 3.7A) (24). MIG expresses GFP so that infection efficiency can be monitored by GFP fluorescence (Figure 3.7A). A second vector containing the PAC gene was also constructed ($MIG_{PAC}$; Figure 3.7B) and results in a bicistronic mRNA in which both PAC and GFP can be translated (Figure 3.7B).

Flow cytometry was used to examine both the infection efficiency and confirm the ability to perform puromycin-based enrichment. After infection with the MIG or $MIG_{PAC}$ vectors, 5.0% and 4.3% of the D9 cells were infected and alive based

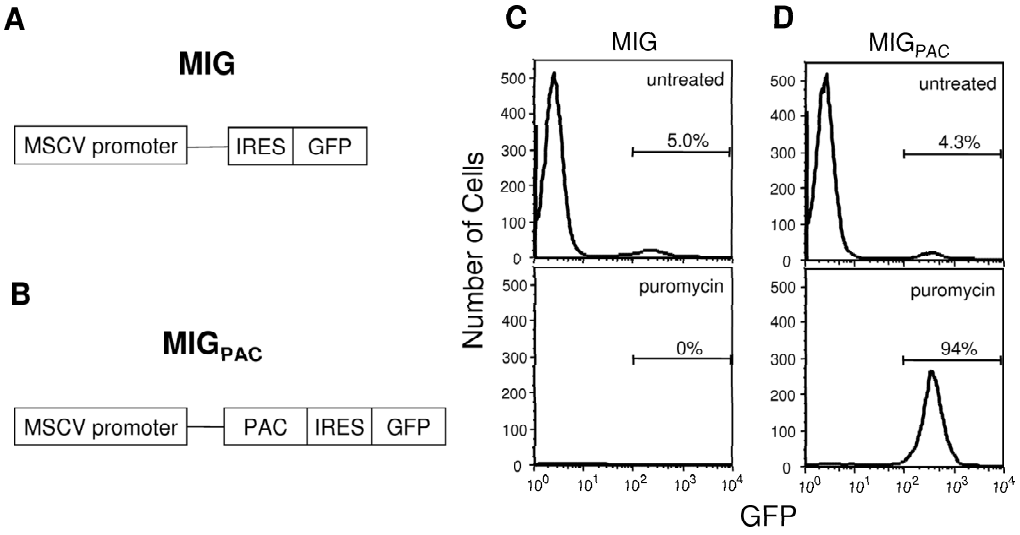


Figure 3.7: Mechanism of action of puromycin in D9 thymocyte cells infected with MIG (A) and $MIG_{PAC}$ (B) constructs. Cells infected with MIG are sensitive (C) and $MIG_{PAC}$ are resistant (D) to puromycin action.

on GFP expression, respectively (Figure 3.7C,D; upper panels). In both cases, the other 95% of the cells showed no GFP-based signal. Puromycin was then added to both MIG and $MIG_{PAC}$ infected cells followed by incubation for 48 h at 37 °C. For MIG infected cells, puromycin results in almost complete killing of both GFP-positive and GFP-negative cells (Figure 3.7C; lower panel). For $MIG_{PAC}$ infected cells, puromycin selectively kills only those cells lacking GFP, such that after 48 hours the population is completely dominated by GFP-positive cells (94%) (Figure 3.7D; lower panel). Enrichment of GFP-positive cells occurs because they express the PAC resistance protein that acylates puromycin, rendering it inactive. These experiments demonstrate that puromycin acylation is sufficient to rescue cells from puromycin toxicity and that *N*-blocked puromycin is non-toxic to D9 cells. The selective enrichment of PAC-expressing cells argues that puromycin exerts its effect on D9 cells by acting on the translation apparatus *in vivo*.

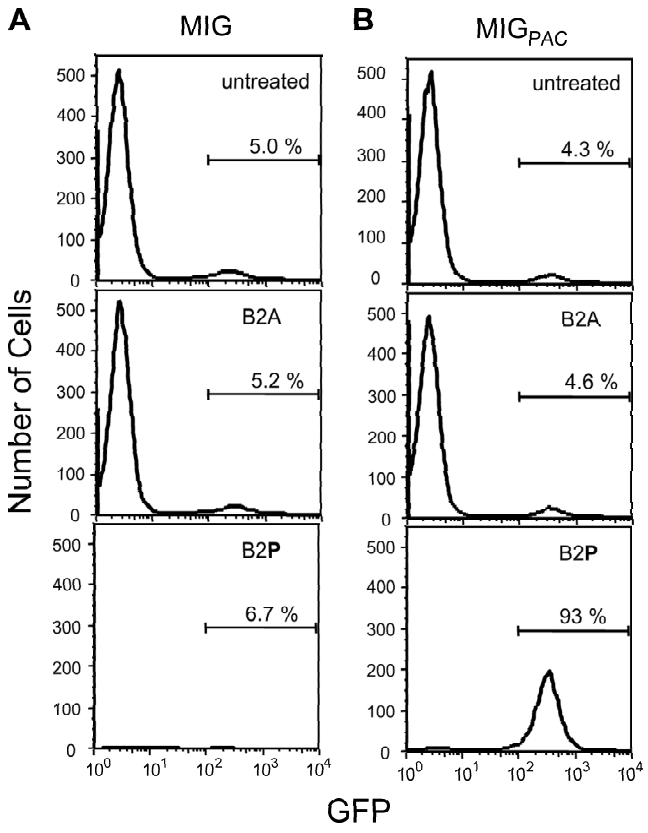


Figure 3.8: Mechanism of action of puromycin conjugates in D9 thymocyte cells. Cells infected with (A) MIG or (B) $MIG_{PAC}$ were treated with biotinylated-puromycin conjugates B2A (**7**) and B2**P** (**6**), both at 25 $\mu$M.

We next wished to examine if B2**P** (**6**) could act in a biochemically similar fashion as puromycin itself. As with puromycin, flow cytometry indicated that long exposures of B2**P** (**6**) kills the vast majority of the cells infected with MIG (Figure 3.8A; bottom panel), while B2A (**7**), a control molecule lacking the amino acid, had no effect (Figure 3.8A; middle panel). Importantly, cells infected with $MIG_{PAC}$ show selective enrichment when incubated with B2**P** (**6**) (Figure 3.8B; bottom panel), while B2A shows no change in GFP-positive and negative populations (Figure 3.8B; middle panel). These experiments are fully consistent with B2**P** (**6**) acting by the same mech-

anism as puromycin itself. Further, these data also provide the first demonstration that PAC can act on puromycin conjugates bearing 5'-extensions *in vivo*.

In line with this conclusion, two other puromycin conjugates show similar activity with B2**P**. We examined a $Cy_5$-bearing conjugate $Cy_5$2**P** (**1**) and compared its action with an analogous control molecule, $Cy_5$2A (2), using both MIG and $MIG_{PAC}$ infected cells. $Cy_5$ provides a useful spectroscopic handle in this context because its red-shifted fluorescence allows the emission of the conjugate to be unambiguously separated from that of GFP. As with B2**P** versus B2A, MIG-infected cells were insensitive to $Cy_5$2A, while long exposure of $Cy_5$2**P** killed both GFP-positive and negative populations, since they lacked the PAC resistance determinant (data not shown). $Cy_5$2**P** also selectively enriched $MIG_{PAC}$ infected cells from 4.3% to 90% (data not shown). Additionally, B2**P**-Me (**11**) also resulted in selective enrichment of MIGPAC-bearing cells and had similar potency with B2**P** (**6**) (data not shown). Taken together, these data support the idea that our various X-dC-puromycin conjugates act by the same mechanism as puromycin *in vivo* and that conjugates lacking the 3'-amino acid moiety have no effect.

### 3.2.5 Western Blot Analysis of Puromycin Conjugate Labeling in Live Cells

Action of puromycin and our conjugates should result in proteins bearing these compounds at their C-terminus *in vivo*. We chose to use Western blot analysis of cellular lysates to examine if incorporation occurred *in vivo* and compare the resulting signal with our control conjugates. Cells were incubated with either BF2**P** (**8**) or the control molecule BF2A (**9**), washed, and a whole-cell lysate was prepared for each sample (see Experimental Procedures). Proteins were run on a SDS-PAGE gel and transferred to nitrocellulose. Equal protein loading was confirmed in each lane using Ponceau S (data not shown). The Ponceau S stain was rinsed away and the blot was probed with an anti-fluorescein antibody to detect any fluorescein-conjugated protein containing

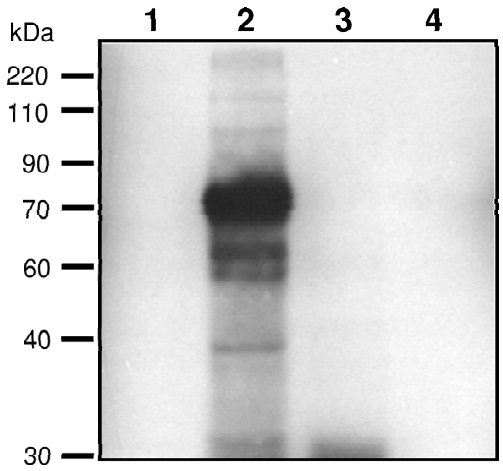


Figure 3.9: Western blot analysis of D9 thymocyte cells treated with a puromycin conjugate and analyzed using an $\alpha$-fluorescein antibody: Lane 1, untreated cells; lane 2, BF2**P**, **8** (25 $\mu$M); lane 3, BF2A, **9** (25 $\mu$M); and anisomycin (250 ng/mL). Ponceau S stain was used to confirm equal protein loading. BF2**P**-conjugated protein is seen at many molecular weights indicating that the conjugate could target all translating ribosomes.

BF2**P** or BF2Λ. Cells treated with BF2**P** (Figure 3.9; lane 2) show good levels of incorporation in this assay, while lanes with cells alone (lane 1), cells treated with BF2Λ (lane 3), or anisomycin (lane 4) show essentially no signal (Figure 3.9). The Western-blot analysis of BF2**P** thus shows good correlation with flow cytometry data and is consistent with a model where puromycin conjugates are stably incorporated into proteins *in vivo* during protein synthesis.

### 3.2.6 Imaging of NIH 3T3 Cells Treated with Fluorescent Puromycin Conjugates

Adherent cells, such as NIH 3T3 cells, allow for spatial resolution of fluorescent molecule localization using fluorescent confocal microscopy. NIH 3T3 cells were treated with various fluorescent puromycin conjugates and imaged to ascertain the regions of conjugate localization (Figure 3.10). Cells were preincubated with anisomycin to inhibit translation and then incubated with either FB2**P** (**3**) or BF2**P** (**8**). Fluorescent confocal images clearly show that samples preincubated with anisomycin followed by incubation with either FB2**P** or BF2**P** (Figure 3.10Λ,C) have lower levels of fluorescence relative to samples not preincubated with anisomycin (Figure 3.10B,D). The images indicate that fluorescent puromycin conjugates localize in the cytoplasm, predominantly outside the nuclear membrane. NIH 3T3 cells were also treated with $Cy_3$2**P** (**1**) and imaged using fluorescent confocal microscopy (Figure 3.11). This shows the same pattern of conjugate localization as seen with FB2**P** and BF2**P** above. These results confirm that fluorescent puromycin conjugates enter cells and label protein during rounds of translation.

## 3.3 Discussion

In the present study, we developed a technique to detect protein synthesis in live cells that does not require gene transfection or radiolabeling. Our strategy thus provides

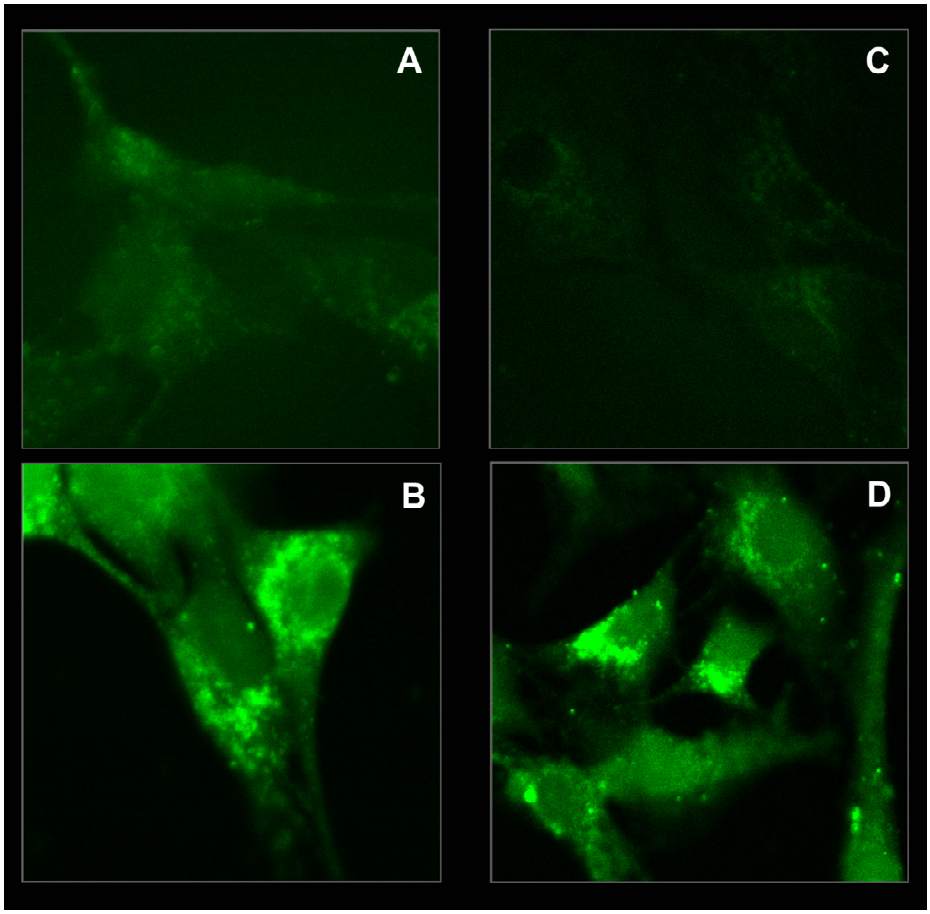


Figure 3.10: Fluorescent confocal microscopy of NIH 3T3 cells treated with 25 $\mu$M FB2**P** (**3**) and 25 $\mu$M BF2**P** (**8**)with (A and C) and without (B and D) anisomycin preincubated.

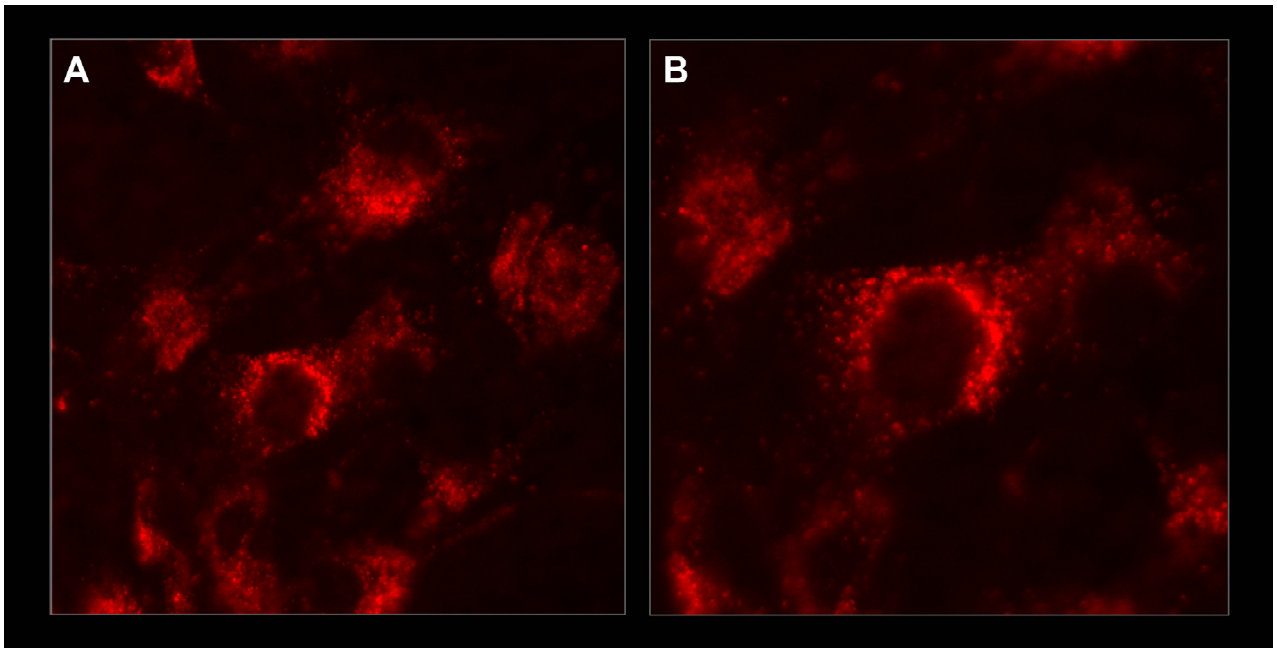


Figure 3.11: Fluorescent confocal microscopy of NIH 3T3 cells treated with $Cy_3$2**P** (**1** at 7.5 $\mu$M). Panel B is higher magnification of a cell in panel A.

an important potential alternative to these methods for studying protein expression *in vivo*. Generally, a great diversity of reagents of the class X-dC-puromycin, where X can be one or two fluorescent or affinity tags, can be constructed and show good activity in protein synthesis *in vitro* and *in vivo*. These reagents all appear to act by the same basic mechanism, entering the ribosomal peptidyl transferase site during translation, followed by covalent attachment to proteins being actively synthesized. Ribosome entry and attachment occurs predominantly at a few discrete sites in the open reading frame including the stop codon, rather than at every position in the chain (25). Previous work also demonstrates that over a 50-fold concentration range that brackets the $IC_{50}$, the length of truncated products is the same and that shorter products are favored as the conjugate concentration is increased substantially.

Despite the intermediate size of these molecules (1163 – 1730 Da), all the conjugates appear to be competent to enter the D9 suspension tissue culture cells used here and act at modest concentrations ($5 - 25\,\mu$M). Experiments with other mammalian and insect cell types support the idea that the ability of these compounds to cross membranes and act in protein synthesis is a general phenomenon (W. B. Smith, E. Schuman, B. Hay, unpublished observations). All of the conjugates we have examined show a significant and measurable shift in the fluorescence intensity of live cells as compared to the control conjugates. Western analysis and selective enrichment studies support the idea that this shift is due to the specific covalent attachment of the conjugates to nascent proteins during translation. Demonstration that affinity tags may be inserted into expressed proteins *in vivo* provides the future opportunity to examine protein expression in response to various cellular stimuli and subsequent identification of the individual polypeptides through a combination of affinity purification and mass spectrometry-based sequence analysis.

In the short term (~24 hours), these compounds are non-toxic based on the proportion of live cells seen in our flow cytometry experiments. The robust labeling and signal to noise we observe thus makes these compounds useful for a great diversity of

cell, tissue, and organism-level experiments. The long-term toxicity of the present set of compounds may provide some limitations for their use. In that context, non-toxic variants that can be photoactivated or presented as pro-drugs may provide useful paths for future conjugate development. The general class of compounds described here should therefore serve as useful cell biology tools to evaluate *in vivo* protein synthesis in areas such as nuclear protein synthesis (26, 27), neuron dentritic protein synthesis (10), dendritic cell aggresome-like induced structures (DALIS) (28), and other novel proteome functions.

## 3.4 Significance

Existing methods to study *in vivo* protein synthesis generally require choice of a candidate gene, radioactivity, or the destruction of cells. To overcome these limitations, we have developed a new class of reagents that enable detection of protein synthesis in live cells using fluorescent and biotinylated puromycin conjugates. These reagents, of the general form X-dC-puromycin, are active *in vitro* and *in vivo* and provide a non-toxic alternative for the study of protein synthesis in live cells. A wide variety of detection moieties appear to be accommodated at the X-position allowing for facile custom reagent design and development. Initial *in vitro* studies correlate the function of our compounds in peptide bond formation during protein synthesis. Subsequent *in vivo* experiments in a mouse thymocyte cell line demonstrate the usefulness of these molecules as indicators of protein synthesis in live cells. Selective enrichment studies with several conjugates as well as Western analysis demonstrate that these compounds all label protein in cells by the same general mechanism, attachment to nascent proteins during translation. The present results thus provide evidence that puromycin conjugates may serve as an alternative to existing tools to elucidate the proteome.

## 3.5 Experimental Procedures

### 3.5.1 Reagents and Materials

L-Puromycin hydrochloride, rabbit globin mRNA, and carboxypeptidase Y (CPY) were obtained from Sigma Chemical Co. (St. Louis, MO). Rabbit reticulocyte Red Nova lysate was purchased from Novagen (Madison, WI). L-[$^{35}$S]methionine ([$^{35}$S]Met) (1175 Ci/mmol) was obtained from NEN Life Science Products (Boston, MA). Immunopure immobilized Neutravidin-agarose was from Pierce (Rockford, IL). GF/A glass microfiber filters were from Whatman. The PAC gene was a kind gift from Joel Pomerantz and David Baltimore.

### 3.5.2 Puromycin Conjugates

Puromycin conjugates were synthesized using standard phosphoramidite chemistry at the California Institute of Technology oligonucleotide synthesis facility. Puromycin-CPG was obtained from Glen Research (Sterling, VA). Oligonucleotides were synthesized with the 5'-trityl intact, desalted via OPC cartridge chromatography (Glen Research) (DNA oligonucleotides only), cleaved, and evaporated to dryness. 5'-Biotin phosphoramidite, Biotin phosphoramidite, 5'-Fluorescein phosphoramidite, 6-Fluorescein phosphoramidite (Glen Research) were used to make the biotin- and dye-puromycin conjugates. Ac-dC-Me-phosphonamidite (Glen Research) was used to prepare the phosphonate puromycin conjugates. The dried samples were resuspended and desalted on Sephadex G-25 (Sigma). Puromycin, puromycin-conjugate, and control molecule concentrations were determined with the following extinction coefficients ($M^{-1}cm^{-1}$): puromycin ($\epsilon_{260}$ = 11,790; in $H_2O$); B2**P** and B2**P**-Me ($\epsilon_{260}$= 19,100; in $H_2O$); F2**P**, F2**P**-Me, DMT-F2**P**-Me, FB2**P**, BF2**P**, F2A, and BF2A ($\epsilon_{471} = 66,000$; in 1X PBS); $Cy_3$2**P** $\epsilon_{650} = 150,000$; in 1X PBS), $Cy_5$2**P** and $Cy_5$2A ($\epsilon_{650} = 250,000$; in 1X PBS).

### 3.5.3 *In Vitro* Potency Determination for Puromycin Conjugates

Translation reactions containing [$^{35}$S]Met were mixed in batch on ice and added in aliquots to microcentrifuge tubes containing an appropriate amount of puromycin-conjugate (or control molecule) dried in vacuo. Typically, a 20 $\mu$l translation mixture consisted of 0.8 $\mu$L of 2.5 M KCl, 0.4 $\mu$L of 25 mM MgOAc, 1.6 $\mu$L of 12.5X translation mixture without methionine, (25 mM dithiothreitol (DTT), 250 mM HEPES (pH 7.6), 100 mM creatine phosphate, and 312.5 $\mu$M of 19 amino acids, except methionine), 3.6 $\mu$L of nuclease-free water, 0.6 $\mu$L (6.1 $\mu$Ci) of [$^{35}$S]Met (1175 Ci/mmol), 8 $\mu$L of Red Nova nuclease-treated lysate, and 5 $\mu$L of 0.05 $\mu$g/$\mu$L globin mRNA. Inhibitor, lysate preparation (including all components except template), and globin mRNA were mixed simultaneously and incubated at 30 °C for 60 min. Each reaction (2 $\mu$L) was combined with 8 $\mu$L of tricine loading buffer (80 mM Tris-Cl (pH 6.8), 200 mM DTT, 24% (v/v) glycerol, 8% sodium dodecyl sulfate (SDS), and 0.02% (w/v) Coomassie blue G-250), heated to 90 °C for 5 min, and applied entirely to a 4% stacking portion of a 16% tricine-SDS-polyacrylamide gel containing 20% (v/v) glycerol (29)(30 mA for 1h, 30 min). Gels were fixed in 10% acetic acid (v/v) and 50% (v/v) methanol, dried, exposed overnight on a PhosphorImager screen, and analyzed using a Storm PhosphorImager (Molecular Dynamics).

### 3.5.4 Neutravidin Capture of *In Vitro* Translated Protein-puromycin-conjugate Products

Neutravidin-agarose [50% slurry (v/v)] was washed 3 times with 1X PBS + 0.1% Tween-20 and resuspended in 1 mL of 1X PBS + 0.1% Tween-20. To 200 $\mu$L of this suspension, 12 $\mu$L of the reaction lysate and 0.8 mL of 1X PBS + Tween-20 were added. The samples were rotated at 4 °C for 3 h and washed with 1X PBS + Tween-20 until the CPM of [$^{35}$S]Met were $< 500$ in the wash. The amount of immobilized

[$^{35}$S]Met-protein-puromycin conjugate was determined by scintillation counting of the Neutravidin-agarose beads.

### 3.5.5 Preparation of $MIG_{PAC}$ Infected 16610D9 Cells

The PAC gene was cloned into MIG using BgII and EcoRI restriction sites to yield $MIG_{PAC}$. 293T-HEK fibroblasts (American Tissue Culture Collection) were co-transfected with pECL-Eco (30) and MIG or $MIG_{PAC}$ by calcium phosphate precipitation. After 12 hours, the precipitate was removed, cells were washed once with PBS, and 4 mL of fresh complete Dulbecco's Modified Eagle Medium (DMEM) supplemented with 10% fetal calf serum (FCS). Viral supernatant was removed 24 hours later and used in infection of 16610D9 cells. One million D9 cells were spin-infected with 0.4 mL of viral supernatant suplemented with 5 $\mu$g/ml Polybrene (Sigma-Aldrich).

### 3.5.6 Enrichment of GFP(+) 16610D9 Cells using Puromycin and Puromycin Conjugates

16610D9 cells infected with either MIG of $MIG_{PAC}$ were cultured in RPMI media with 10% FBS and grown at 37 °C in a humidified atmosphere with 5% $CO_2$. For each experiment, 16610D9 cells (0.25 x $10^6$/well) were added to 24-well microtiter plates along with puromycin, puromycin-conjugate, and control molecules dissolved in the minimum amount of either media or PBS. After a 48 h incubation, the cells were washed twice in 2 mL PBS + 4% FCS and resuspended in PBS + 4% FCS supplemented with 2% formaldehyde along with incubation at 37 °C for 10 min. Flow cytometry was carried out on a Beckman FACScabilur Flow Cytometer.

### 3.5.7 Detection of Protein Synthesis Events *In vivo* using Flow Cytometry

16610D9 cells (0.5 million $mL^{-1}$) were combined with the various puromycin conjugates and control molecules resuspended in the minimum volume of PBS or media as described above. After a 24 h incubation, the cells were washed twice in 2 mL PBS + 4% FCS and resuspended in PBS + 4% FCS supplemented with 2% formaldehyde followed by incubation at 37 °C for 10 min or used directly after washing for immediate flow cytometry analysis.

### 3.5.8 Western Blot Analysis of 16610D9 Cells Treated with Puromycin Conjugates

Cells were prepared as described above except as indicated anisomycin was added to a final concentration of 250 $\mu$g $mL^{-1}$ and washed twice in PBS. Live cell number was determined using trypan blue exclusion dye and each sample was adjusted to contain an equal number of live cells. Cell pellets were resuspended in 2X lysis buffer (100 mM $\beta-$glycerophosphate, 3 mM EGTA, 2 mM EDTA, 0.2 mM sodium-orthovanadate, 2 mM DTT, 20 $\mu$g/ml aprotinin, 20 $\mu$g/ml leupeptin, 50 $\mu$g/ml trypsin inhibitor, and 4 $\mu$g/ml pepstatin, and 1% Triton X-100) and incubated on ice for 30 min. Cell debris was removed by centrifugation at 20,000 x g for 30 min. Cell lysate was combined with SDS loading buffer (0.12 M Tris-Cl (pH 6.8), 20% glycerol, 4% (w/v) SDS, 2% (v/v) $\beta-$mercaptoethanol, and 0.001% bromophenol blue) and heated at 90 °C for 10 min. Samples were applied entirely to a 4% stacking portion of a 10% glycine-SDS-polyacrylamide gel (30 mA for 1h, 30 min). Protein was transferred using standard Western transfer transfer techniques and the blot was probed with an anti-fluorescein antibody followed by an anti-rabbit-horseradish peroxidase conjugate (Pierce chemicals). The chemiluminescence reaction was carried out using the ECL PLUS Western Blotting Detection System (Amersham Biosciences).

### 3.5.9 Confocal Microscopy of NIH 3T3 cells Treated with Fluorescent Puromycin Conjugates

NIH 3T3 cells were plated (50,000 cells/slide) on glass bottom cell culture imaging chambers. After 24 h, cells were preincubated with anisomycin in a total volume of 400 $\mu$L (50 $\mu$M) for 4 h. The cells were incubated with the fluorescent puromycin conjugates in a total volume of 400 $\mu$L (resuspended in media) for 7 h. After washing the cells 4 times with 1X PBS and adding a HEPES-buffered solution, images were collected on a Zeiss LSM 510-META confocal microscope using a 63X oil immersion lens.

## Acknowledgements

We gratefully acknowledge the help and useful discussions from our collaborators Erin Schuman, W. Bryan Smith, and Bruce Hay who have examined puromycin-dye conjugates in various *in vivo* systems. This work was supported by NIH Grant R01 GM60416 to R.W.R. and by NIH training grant GM 07616 (S.R.S.).

# References

[1] The International Human Genome Sequencing Consortium. Initial sequencing and analysis of the human genome. *Nature*, 409:860–921, 2001.

[2] J.C. Venter, M.D. Adams, E.W. Myers, P.W. Li, R.J. Mural, G.G. Sutton, H.O. Smith, M. Yandell, C.A. Evans, and R.A. et al. Holt. The sequence of the human genome. *Science*, 291:1304–1351, 2001.

[3] R.F. Duncan, H. Peterson, C.H. Hagedorn, and A. Sevanian. Oxidative stress increases eukaryotic initiation factor 4E phosphorylation in vascular cells. *Biochem. J.*, 369:213–225, 2003.

[4] J.H. Lipschutz, V.R. Lingappa, and K.E. Mostov. The exocyst affects protein synthesis by acting on the translocation machinery of the endoplasmic reticulum. *J. Biol. Chem.*, 278:20954–20960, 2003.

[5] C. Constantinou, M. Bushell, I.W. Jeffrey, V. Tilleray, M. West, V. Frost, J. Hensold, and M.J. Clemens. p53-induced inhibition of protein synthesis is independent of apoptosis. *Euro. J. Biochem.*, 270:3122–3132, 2003.

[6] D.L. Lockhart and E.A. Winzeler. Genomics, gene expression and DNA arrays. *Nature*, 405:827–836, 2000.

[7] P. van Roessel and A.H. Brand. Imaging into the future: Visualizing gene expression and protein interactions with fluorescent proteins. *Nat. Cell Biol.*, 4, 2003.

[8] A. Miyawaki, J. Llopis, R. Heim, J.M. McCaffery, J.A. Adams, M. Ikura, and R.Y. Tsien. Fluorescent indicators for $Ca^{2+}$ based on green fluorescent proteins and calmodulin. *Nature,* 288:882–887, 1997.

[9] A.Y. Ting, K.H. Kain, R.L. Klemke, and R.Y. Tsien. Genetically encoded fluorescent reporters of protein tyrosine kinase acitivities in living cells. *Proc. Natl. Acad. Sci. U.S.A.*, 98:15003–15008, 2001.

[10] O. Steward and E.M. Schuman. Protein synthesis at synaptic sites on dendrites. *Annu. Rev. Neurosci.*, 24:299–325, 2001.

[11] G. Aakalu, W.B. Smith, N. Nguyen, C.G. Jiang, and E.M. Schuman. Dynamic visualization of local protein synthesis in hippocampal neurons. *Neuron*, 30:489–502, 2001.

[12] D. Nathans. Puromycin inhibition of protein synthesis: incorporation of puromycin into peptide chains. *Proc. Natl. Acad. Sci. U.S.A.*, 51:585–592, 1964.

[13] M.B. Yarmolinsky and G. de la Haba. Inhibition by puromycin of amino acid incorporation into protein. *Proc. Natl. Acad. Sci. U.S.A.*, 45:1721–1729, 1959.

[14] N. Doi, H. Takashima, M. Kinjo, K. Sakata, Y. Kawahashi, Y. Oishi, R. Oyama, E. Miyamoto-Sato, T. Sawasaki, Y. Endo, and H. Yanagawa. Novel fluorescence labeling and high-throughput assay technologies for *in vitro* analysis of protein interactions. *Genome Res.*, 12:487–492, 2002.

[15] Y. Kawahashi, N. Doi, H. Takashima, C. Tsuda, Y. Oishi, R. Oyama, M. Yonezawa, E. Miyamoto-Sato, and H. Yanagawa. *In vitro* protein microarrays for detecting protein-protein interactions: Application of a new method for fluorescence labeling of proteins. *Proteomics*, 3:1236–1243, 2003.

[16] N. Nemoto, E. Miyamoto-Sato, Y. Husimi, and H. Yanagawa. *In vitro* virus: Bonding of mRNA bearing puromycin at the 3'-terminal end to the C-terminal

end of its encoded protein on the ribosome *in vitro*. *FEBS Lett.*, 414:405–408, 1997.

[17] S.R. Starck and R.W. Roberts. Puromycin oligonucleotides reveal steric restrictions for ribosome entry and multiple modes of translation inhibition. *RNA*, 8:890–903, 2002.

[18] S.R. Starck, X. Qi, B.N. Olsen, and R.W. Roberts. The puromycin route to assess stereo- and regiochemical constraints on peptide bond formation in eukaryotic ribosomes. *J. Am. Chem. Soc.*, 125:8090–8091, 2003.

[19] *In Living Color: Protocols in Flow Cytometry and Cell Sorting*. Springer-Verlag: Berlin, 2000.

[20] L. Van Parijs, Y. Refaeli, J.D. Lord, B.H. Nelson, A.K. Abbas, and D. Baltimore. Uncoupling IL-2 signals that regulate T cell proliferation, survival, and Fas mediated activation-induced cell death. *Immunity*, 11:281–288, 1999.

[21] S. de la Luna and J. Ortin. Pac gene as efficient dominant marker and reporter gene in mammalian cells. *Methods Enzymol.*, 216:376–385, 1992.

[22] J.N. Porter, R.I. Hewitt, C.W. Hesseltine, G. Krupka, J.A. Lowery, W.S. Wallace, N. Bohonos, and J.H. Williams. Achromycin: A new antibiotic having trypanocidal properties. *Antibiotics and Chemo.*, 11:409–410, 1952.

[23] J.A. Pérez-González, J. Vara, and A. Jiménez. Acetylation of puromycin by *Streptomyces alboniger* the producing organism. *Biochem. Biophys. Res. Commun.*, 113:772–777, 1983.

[24] G. Bain, M.W. Quong, R.S. Soloff, S.M. Hedrick, and C. Murre. Thymocyte maturation is regulated by the activity of the helix-loop-helix protein. *J. Exp. Med.*, 190:1605–1616, 1999.

[25] S.L. Wolin and P. Walter. Ribosome pausing and stacking during translation of a eukaryotic mRNA. *EMBO*, 7:3559–3569, 1988.

[26] F.J. Iborra, D.A. Jackson, and P.R. Cook. Coupled transcription and translation within nuclei of mammalian cells. *Science*, 293:1139–1142, 2001.

[27] L. Nathanson, T. Xia, and M.P. Deutscher. Nuclear protein synthesis: a re-evaluation. *RNA*, 9:9–13, 2003.

[28] H. Lelouard, V. Ferrand, D. Marguet, J. Bania, V. Camosseto, A. David, E. Gatti, and P. Pierre. Dendritic cell-aggresome-like induced structures are dedicated areas for ubiquitination and storage of newly synthesized defective proteins. *Cell Biol.*, 164:667–675, 2004.

[29] H. Schagger and G.V. von Jagow. Tricine-sodium dodecyl sulfate-polyacrylamide gel electrophoresis for the separation of proteins in the range from 1 to 100 kDa. *Anal. Biochem.*, 166:368–379, 1987.

[30] R.K. Naviaux, E. Costanzi, M. Haas, and I.M. Verma. The pCL vector system: Rapid production of helper-free, high-titer, recombinant retroviruses. *J. Virology*, 70:5701–5705, 1996.